

T. Mergner · G. Nasios · C. Maurer · W. Becker

## Visual object localisation in space

### Interaction of retinal, eye position, vestibular and neck proprioceptive information

Received: 18 December 2000 / Accepted: 5 June 2001 / Published online: 6 September 2001  
© Springer-Verlag 2001

**Abstract** Perceptual updating of the location of visual targets in space after intervening eye, head or trunk movements requires an interaction between several afferent signals (visual, oculomotor efference copy, vestibular, proprioceptive). The nature of the interaction is still a matter of debate. To address this problem, we presented subjects ( $n=6$ ) in the dark with a target (light spot) at various horizontal eccentricities (up to  $\pm 20^\circ$ ) relative to the initially determined subjective straight-ahead direction (SSA). After a memory period of 12 s in complete darkness, the target reappeared at a random position and subjects were to reproduce its previous location in space using a remote control. For both the presentation and the reproduction of the target's location, subjects either kept their gaze in the SSA (retinal viewing condition) or fixated the eccentric target (visuo-oculomotor). Three experimental series were performed: A, "visual-only series": reproduction of the target's location in space was found to be close to ideal, independently of viewing condition; estimation curves (reproduced vs presented positions) showed intercepts  $\approx 0^\circ$  and slopes  $\approx 1$ ; B, "visual-vestibular series": during the memory period, subjects were horizontally rotated to the right or left by  $10^\circ$  or  $18^\circ$  at 0.8-Hz or 0.1-Hz dominant frequency. Following the 0.8-Hz body rotation, reproduction was close to ideal, while at 0.1 Hz it was partially shifted along with the body, in line with the known vestibular high-pass characteristics. Additionally, eccentricity of target presentation reduced the slopes of the estimation curves (less than 1); C, "visual-vestibular-neck series": a shift toward the

trunk also occurred after low-frequency neck stimulation (trunk rotated about stationary head). When vestibular and neck stimuli were combined (independent head and trunk rotations), their effects summed linearly, such that the errors cancelled each other during head rotation on the stationary trunk. Variability of responses was always lowest for targets presented at SSA, irrespective of intervening eye, head or trunk rotations. We conclude that: (1) subjects referenced "space" to pre-rotatory SSA and that the memory trace of the target's location in space was not altered during the memory period; and that (2) they used internal estimates of eye, head and trunk displacements with respect to space to match current target position with the memory trace during reproduction; these estimates would be obtained by inverting the physical coordinate transformations produced by these displacements. We present a model which is able to describe these operations and whose predictions closely parallel the experimental results. In this model the estimate of head rotation in space is not obtained directly from the vestibular head-in-space signal, but from a vestibular estimate of the kinematic state of the body support.

**Keywords** Spatial representation · Reference frames · Vestibular-propriceptive interaction · Object localisation · Model · Human

## Introduction

When we evaluate the location of a visual object in extra-personal space in the absence of external landmarks (visual, auditory, haptic), we rely on information from different sensory modalities. Using abstract terms, the processing of this information by the CNS can be described as a step-wise coordinate transformation, first from the object's position in retinal coordinates into a craniocentric representation and, ultimately, into a space-centred representation (Andersen et al. 1993). These transformations result from appropriate interactions of

T. Mergner (✉) · G. Nasios · C. Maurer  
Neurologische Klinik, Universität Freiburg,  
Breisacherstr. 64, 79106 Freiburg, Germany  
e-mail: mergner@uni-freiburg.de  
Tel.: +49-761-2705313, Fax: +49-761-2705390

G. Nasios  
Neurological Clinic of Ioannina University,  
45100 Ioannina, Greece

W. Becker  
Sektion Neurophysiologie, Universität Ulm,  
89081 Ulm, Germany

the retinal signal of object-versus-eye position, with an “efference copy” of eye-in-head position and a vestibular signal of head-in-space displacement. The exact nature of these interactions is still a matter of debate.

For example, the results of experiments aiming at elucidating the *retinal-oculomotor interaction* that is involved in the localisation of a visual target in space appear to depend on the motor system used to probe it. Using open-loop finger pointing to visually presented targets, several authors found systematic errors when gaze direction deviated from target direction so that extrafoveal retinal information became involved (Bock 1986; Enright 1995; see Henriques et al. 1998; Lewald and Ehrenstein 2000). Furthermore, pointing in the direction of gaze without target is very inaccurate (Bock 1986). Bock therefore concluded that a complex, non-linear interaction between the two signals is required to achieve an accurate internal representation of space. Matters are also complicated by considerable differences in methodology among laboratories (Mapp et al. 1989; Prablanc et al. 1979). In contrast, open-loop saccadic eye pointing (saccades to the location of a remembered target) is rather accurate, even after intervening eye and head movements (see Karn et al. 1997). This discrepancy between arm and eye pointing probably reflects differences in sensorimotor transformation rather than different intersensory transformations (see Discussion).

In the present study, we sought to eliminate the effect of sensorimotor distortions by using an delayed intrasensory match-to-sample paradigm and a remote control for the response. Our subjects were to reproduce the location of a previously presented light spot in space by repositioning this spot after it had changed position during an intervening memory period, a task that, unlike pointing procedures, can circumvent the use of body-centred coordinates. The mode of retinal-oculomotor interaction was addressed by using two different target viewing conditions for both the presentation and the reproduction of target location in a cross-over design: in one condition gaze and target position were dissociated (peripheral viewing), whereas in the second condition they coincided. By evaluating, in addition to the mean response accuracy, response variability, we obtained clues revealing how subjects combine retinal and eye position signals to construct a memory map of target position in space.

It has repeatedly been shown that *interaction with vestibular input* is required to maintain a correct memory of spatial target position (possibly in body-centred coordinates) during body rotation. For example, saccades to the spatial location of a target presented prior to a horizontal rotation are quite accurate (Bloomberg et al. 1988; Israel and Berthoz 1989). However, such saccades fall short when the frequency or angular velocity of the body rotation is low (Mergner et al. 1998). Analogous errors have been observed for object motion perception (Mergner et al. 1992) and updating of target location (Maurer et al. 1997) in space-centred coordinates. These errors reflect both the known high-pass characteristics of the semicircular canal system (see Fernandez

and Goldberg 1971) and the high detection threshold of human self-motion perception (Mergner et al. 1991). Taken together, the findings suggest that vestibular signals interact with retinal and oculomotor signals by way of a linear summation.

This linear summation hypothesis has been challenged, however, in a number of studies by Blouin et al. (1997, 1998a, 1998b), who observed systematic errors when pre-rotatory target position was eccentric with respect to the head (in the aforementioned studies, it always was straight ahead prior to rotation). We therefore extended our study and subjected our subjects also to body rotations during the memory period with the aim of comparing the post-rotatory localisation of targets that, prior to rotation, had been presented at both centric and various eccentric positions with respect to the head.

In contrast to what is observed during whole-body rotation, visual targets presented in head-centric position are veridically localised after an intervening isolated head rotation about the stationary trunk (combination of vestibular and *neck proprioceptive input*), even if head rotation is slow (Maurer et al. 1997; Mergner et al. 1998). These studies and related work (overviews: Mergner et al. 1997; Mergner and Rosemeier 1998) show that *vestibular-neck interaction* is optimised for the behavioural condition of head rotation on stationary trunk (broad-band instead of high-pass characteristics, low instead of high detection threshold). On the assumption that pre-rotatory target-versus-head eccentricity would cause errors of the type reported by Blouin et al. (1997, 1998a, 1998b), we wondered whether a comparison across different vestibular-neck stimulus combinations might help to identify their source. Furthermore, focusing not only on mean localisation error, but also analysing the response variability arising with vestibular-neck interaction, we investigated whether an optimisation for behavioural conditions can be verified also in terms of the susceptibility to internal “noise” (i.e. whether the scatter of localisation errors reaches a minimum when only the head is rotated).

---

## Methods

With approval of the local ethics committee, six healthy subjects (four men and two women; mean age  $\pm$  SD, 35.8 $\pm$ 9.3 years) were studied. All of them gave their informed consent. Integrity of subjects’ vestibular function was ascertained with conventional electronystagmography. The methods described in the following sections were originally developed in a previous study by Maurer et al. (1997).

### Apparatus

Subjects were seated on a Bárány chair. Each subject’s head was coupled, by means of a dental bite-board, to a head holder, which was mounted on the chair and could be rotated about the same axis as the chair. Chair and head holder were driven by two independent servomotors under computer control, which served also to match their dynamics. The chair was surrounded by a cylindrical screen (radius 1 m) onto which a red spot (“target”; luminance,

≈20 cd/cm<sup>2</sup>; diameter, 0.5° of visual angle) was projected, at the subject's eye level, by means of a mirror galvanometer mounted above the subject's head and positioned in line with the chair axis.

The galvanometer received three input signals for the following 3 functions:

1. Target presentation. In the course of each trial, a computer-generated signal stepped the target by a given amount (0°, 4°, 8°, 12°, 16° or 20°) to the right or left side. Subjects were to remember the resulting location in space.
2. Indication. The same light spot that served as target also served as probe by which subjects indicated an instructed direction or the remembered target position. For its adjustment, subjects used a hand-held potentiometer (joystick). Using this remote control largely prevented distortions related to subjects' motor performance (Maurer et al. 1997).
3. "Indication sequence". Each time subjects had adjusted the spot for the indication, a computer-generated signal disturbed the indication, stepping the spot by 8° to either the right or left of the indicated position, so that subjects were forced to repeatedly readjust its position ( $n=6$ ; intervals, 2.5 s; direction varied in pseudo-random order to balance for a hysteresis in subjects' adjustment performance; see Maurer et al. 1997).

During stepping, the spot was always extinguished in order to avoid visual motion cues. Because its luminance was low and because it did not remain stationary for long periods, no relevant afterimages occurred.

#### Stimuli and procedures

Prior to each experiment, the head holder was adjusted so as to align subjects' heads with their sagittal torso axis. Subjects then were asked to indicate with the help of the light spot their subjective straight-ahead direction while the room was illuminated. This indication served as a reference for their later indications of subjective straight ahead in the dark (SSA). Thereafter, the experimental trials were started, which consisted of 5 parts (see examples in Fig. 1):

- i) Indication of the SSA. At the beginning of each trial the room lights were extinguished and subjects were presented with the target at a random position in space. By means of the joystick they aligned the target with their SSA direction. Once aligned, the indication sequence commenced, forcing subjects to re-adjust it 6 times in all. Thereafter, subjects remained in complete darkness for one second.
- ii) Target presentation period. The target was offset by an eccentricity of 0°, 4°, 8°, 12°, 16° or 20° to the right or left with respect to the last indication of SSA determined in step 1 and was presented for 3 s before being extinguished. Subjects were asked to attend to and to memorise its *spatial* location for reproduction during step iv.
- iii) Memory period. During the subsequent 12 s, subjects remained in complete darkness. During this time either:
  - A. The chair was kept stationary ("visual-only series")
  - B. The chair was rotated to the right or left side ("visual-vestibular series")
  - C. Both chair and head holder were rotated in various combinations ("visual-vestibular-neck series"). Subjects were instructed to keep gaze straight in their heads during iii (and vi), in order to minimise lasting eye deviations which are known to produce shifts of SSA (see Howard 1982).
- iv) Reproduction period. The target reappeared at a random position in space and subjects were to restore its previous spatial location. In the following we refer to the target in the context of reproduction as the "probe" that had to be matched to the remembered location of the target. During the following indication sequence, the indication was repeated six times.
- v) Waiting period. When step 3 involved rotational stimuli (series B and C), the chair and the head holder were rotated back to their primary positions. The screen then was illuminated, and

subjects released their heads from the bite board to perform moderate head shaking and to reorient in space.

#### Viewing conditions

During target presentation, subjects were to use two different viewing conditions:

1. Retinal (RET) viewing. Subjects were to maintain gaze in SSA direction (Fig. 1a, traces b, c; b, trace b) so that the target would fall on the peripheral retina.
2. Visuo-oculomotor (VOM) viewing. Subjects were to gaze at the target so that it would be viewed with zero retinal eccentricity (Fig. 1a, traces a, d; b, trace a). After extinction of the target, at the beginning of the memory period, they were to look back into SSA direction. Thus, the eye was displaced prior to the reproduction period.

Likewise, during reproduction of the target's spatial position, subjects either maintained gaze in SSA direction (RET reproduction; Fig. 1a, traces c, d) or fixated at the target (VOM reproduction; Fig. 1a, traces a, b; b, traces a, b).

#### Experimental series

##### *Series A: visual-only series*

This series comprised four different runs, each with a different combination of the viewing conditions during presentation and reproduction (VOM/VOM, RET/VOM, RET/RET, VOM/RET). Each run consisted of 10 trials, with each target eccentricity ( $\pm 4$ ,  $\pm 8$ ,  $\pm 12$ ,  $\pm 16$  and  $\pm 20^\circ$ ) occurring once, and was repeated eight times per subject.

##### *Series B: visual-vestibular series*

In this series, five different target eccentricities were used ( $-16^\circ$ ,  $-8^\circ$ ,  $0^\circ$ ,  $+8^\circ$ , and  $+16^\circ$ ). Furthermore, 8 different vestibular stimuli were applied during the memory period, covering the two directions of rotation (left and right with respect to the primary or starting position), two different amplitudes ( $10^\circ$  and  $18^\circ$ ), and two different dominant frequencies (0.8 Hz and 0.1 Hz). Finally, two different combinations of viewing conditions were used in separate runs (VOM/VOM and RET/VOM). Each run comprised 40 trials (5 target eccentricities  $\times$  8 vestibular stimuli) and was repeated three times.

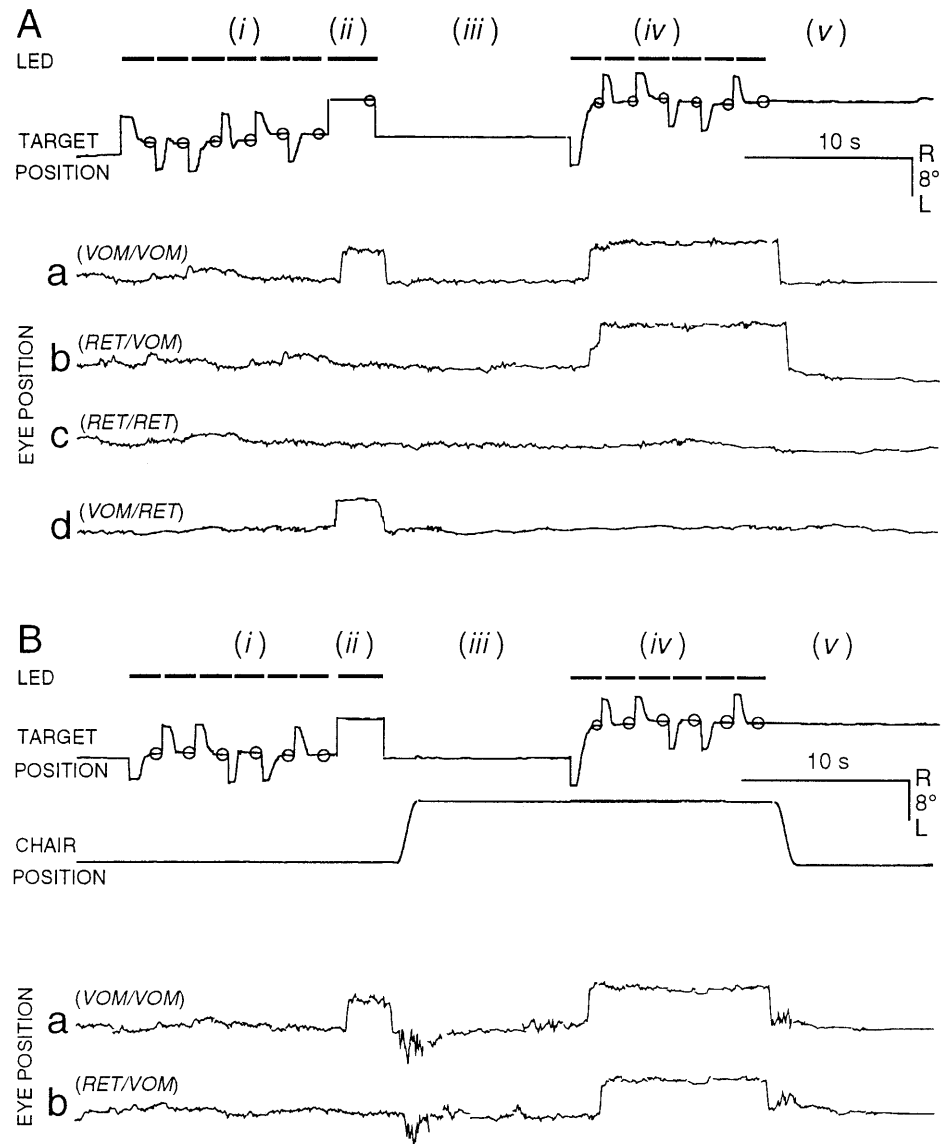
##### *Series C: visual-vestibular-neck series*

There were again five target eccentricities:  $-16^\circ$ ,  $-8^\circ$ ,  $0^\circ$ ,  $+8^\circ$ , and  $+16^\circ$ . During the memory period, one of the following combinations of vestibular and neck stimuli (compare Fig. 4c) was administered:

- Vestibular-only (VEST). As in series B.
- Neck-only (NECK). During chair rotation, the head holder was rotated by the same amount as, but in the opposite direction of the chair; this manoeuvre kept the head stationary in space while the body was rotating.
- Synergistic vestibular-neck combination (VEST+NECK). By rotating the head holder on the stationary chair (trunk), a synergistic vestibular and neck stimulation was created.
- Antagonistic vestibular-neck combination (VEST-NECK). A head-holder rotation was combined with a counter-phase chair rotation of double amplitude. Thus, head-on-trunk (neck stimulus) was opposite to the head-in-space movement (vestibular stimulus).

The amplitudes of the vestibular and neck stimuli in this series always were  $+18^\circ$  or  $-18^\circ$ , unless a particular condition required one of them to be zero. Only one combination of viewing condi-

**Fig. 1a, b** Experimental paradigms used to evaluate the updating of the location of a previously presented visual target in space. **a** Visual-only series (subjects stationary). Traces show examples of target position and eye position (in degrees; traces a–d), with dashed line on top (LED) indicating when target was lit. The trial consisted of 5 parts: (i) indication of the subjective straight-ahead direction, SSA (6 times, interrupted by target steps); (ii) presentation of target with respect to SSA (here at 10° right eccentricity); (iii) memory period, in complete darkness; (iv) reproduction of target location in space (6 times); (v) waiting period in darkness. Traces a–d: Examples of EOG recordings for the four viewing conditions tested (VOM visuo-oculomotor: gaze is shifted on target and, after its extinction, back to primary position; RET retinal: gaze is kept in direction of SSA). Abbreviations give first the viewing condition for target presentation (during ii) and then that for reproduction (iv). Circles on target position trace indicate samples used for analysis. **b** Visual-vestibular series. As in **a**, but during part iii a stimulus (here vestibular, means whole-body rotation of 18° towards the right; dominant frequency,  $f=0.8$  Hz) was applied (back rotation in part v). **a, b** Examples of EOG recordings for the two viewing conditions taken from this series (**a** VOM/VOM; **b** RET/VOM)



tions was used (VOM/VOM). Two runs were performed (dominant frequency of 0.8 Hz and 0.1 Hz), each consisting of 40 trials (5 target eccentricities  $\times$  4 combinations  $\times$  2 directions of rotation). Each run was repeated three times per subject.

The rotational stimuli consisted of ramp-like angular displacements having approximately bell-shaped velocity profiles ("raised cosine" function,  $v(t) = -A \cdot f \cdot \cos(2\pi ft) + A \cdot f$ , where  $t$  is time,  $A$  is angular displacement and  $f$  is frequency). For the 0.8-Hz and 0.1-Hz stimuli, durations amounted to 1.25 s and 10 s, and peak angular velocities to 28.8°/s and 3.6°/s, respectively. The rotation devices used did not generate noticeable noise or vibration. Auditory spatial orientation cues from the apparatus in the room were minimised by plugging subjects' ears.

The order of stimulus presentations and the combinations of viewing conditions, target amplitudes, stimulation amplitudes, vestibular and neck stimuli were always randomised and balanced across repeated runs.

#### Eye movement recordings

Compliance with the instructed viewing instructions was controlled by recording subjects' eye movements (bitemporal conven-

tional DC electro-oculography, EOG) in the first two runs of the experimental series. As shown in Fig. 1, gaze was held rather accurately in SSA direction with RET viewing during target presentation (ii), and it was returned into this direction with VOM viewing after the target had been foveated and extinguished. Furthermore, gaze direction was essentially maintained during the memory period (iii), and this also applied during the reproduction period (iv) with RET viewing. In the VOM reproduction conditions, subjects foveated the probe, but with a particular strategy. After a few trials they generally no longer looked at the location where, at the start of the indication sequence, the light spot first appeared. Rather, they made a saccadic gaze shift straight away (which could comprise secondary, conceivably corrective, saccades) towards the remembered spatial position of the target (see Fig. 1a, traces a, b; b). Typically, this position was maintained throughout the reproduction period, ignoring the repeated displacements of the target by the indication sequence. Small eye movements did occur during the final phases of target adjustments following each inflicted displacement, but these were often below the resolution of our EOG recordings. Yet we like to stress that subjects were performing a matching task, as they ascertained on request, and not an "eye pointing" task (e.g. to remembered target locations), as one might expect from Fig. 1.

## Data acquisition and analysis

The potentiometer readings of the remote control device (joystick), the EOG signal, and an on-off signal of target illumination, were fed into a laboratory computer together with the position readings of the Bárány chair, the head holder, and the galvanometer (sampling rate, 50 Hz). Data were displayed on a computer screen and stored simultaneously on hard disk for off-line analysis. Analysis was performed using an interactive computer program, which automatically marked the last 20 data points that preceded each step displacement of the target (Fig. 1a, b, circles in the “target position” traces); if correctly marked, they were accepted and stored. From these data we evaluated:

- The SSA, by taking the mean value ( $\pm$  SD) across the 2nd–5th indication during part i of an experiment. The target steps for these 4 indications in the pseudorandom indication sequence always contained two target steps to each side; the 1st indication was dismissed, because it showed rather large variations, and the 6th was dismissed for balancing the directions.
- The reproduction of spatial target position (mean reproduction response or accuracy), by calculating the mean value across the 2nd–5th indication in the indication sequence of part iv *relative* to the preceding SSA. Because the signal that stepped the target to the next spatial position (part ii) was superimposed on the 6th indication of SSA rather than on mean SSA (across the four repetitions analysed), a small discrepancy between actual and intended relative target eccentricity resulted, which was post hoc corrected (unlike in a preliminary report, Nasios et al. 1999, which therefore gives slightly different data).
- Across-subjects variability, expressed in terms of the standard deviation (SD) of the population mean.
- Across-trials variability,  $s_{xt}$ , obtained by calculating the SD of each subject’s performance across trial repetitions and averaging these values across subjects.
- Indication variability,  $s_{it}$ , obtained by calculating the intra-trial SD across the 2nd–5th indication in each probe sequence (reproduction). These values then were averaged first across the trial repeats of each subject and finally across all subjects. The same procedure was applied to SSA indications.

In order to prevent instrumental variability from influencing the above measures of response variability, subjects’ responses always were corrected for the difference between the nominal (desired) amplitudes of trunk and head rotation and the effectively achieved amplitudes (which could vary by  $\pm 3\%$  as a result of differing body masses and imperfect gear-drive control). Thus, potentiometer and ADC noise were the only sources of contamination (less than 1%). No corrections were required for galvanometer errors; a slight position non-linearity was irrelevant because it affected probe and target positions in identical ways, and reproducibility of galvanometer deflection was better than  $\pm 0.05^\circ$ .

Note that our measure of mean reproduction accuracy (b) basically corresponds to what others have called “constant” or “systematic” error, while the across-trials variability (d) is related to the “variable” or “absolute” error. Finally, the indication variability (c) was determined in an attempt to decompose the variable error into one related to the “noise” of the memory trace, the other to the variability of perceived probe position and its matching with the memory trace (see Discussion).

Statistics was performed separately for each experimental series, using ANOVA (StatView; Abacus Concepts). Details are given in the context of the results.

## Results

### Visual-only series (A)

The grand mean of SSA (subjective straight ahead in the dark; see Methods) across all subjects and all trials deviated from the reference direction by  $4.3 \pm 1.7^\circ$  (mean  $\pm$

across-subjects SD; towards the right) in the visual-only series. The corresponding indication SD and across-trials SD averaged  $\pm 0.56^\circ$  and  $\pm 1.7^\circ$ , respectively.

Figure 2 shows, for each of the four combinations of viewing conditions, the mean indications of target position as a function of target eccentricity with respect to SSA (vertical bars, across-subjects SD). Subjects’ estimates were almost perfect (data close to  $45^\circ$  lines) when they fixated at the probe during reproduction, irrespective of whether upon presentation they fixated the target (VOM/VOM, Fig. 2a; estimation curve  $y=1.03x+0.08$ ,  $r^2=0.97$ ) or viewed it peripherally (RET/VOM, Fig. 2b;  $y=1.02x+0.35$ ,  $r^2=0.97$ ). On the other hand, with peripheral probe-viewing during reproduction (RET/RET, Fig. 2c; VOM/RET, Fig. 2d), subjects slightly overestimated the target position regardless of the mode of target viewing ( $y=1.1x+0.41$ ,  $r^2=0.94$ , and  $y=1.1x+0.18$ ,  $r^2=0.94$ , respectively). However, a closer scrutiny of the latter data revealed that this overestimation was mainly due to two subjects; their estimation curves exhibited slopes clearly more than 1, while those of the remaining four subjects were close to unity (1.19 and 1.15 versus 1.01 and 1.05 for RET/RET and VOM/RET, respectively). Thus, the slight difference in accuracy between foveal (\*VOM) and peripheral (\*RET) probe viewing cannot be considered significant.

The variability of the successive probe adjustments during a given trial (indication SD,  $s_{it}$ ) did not exhibit a significant dependence on the mode of target viewing, but only on probe viewing [larger with \*/RET than with \*/VOM,  $F=44.25$ ,  $P<0.0001$ ; repeated-measures ANOVA with factors Target viewing (RET, VOM) and Probe viewing mode (also RET, VOM)].  $s_{it}$  with \*/RET increased with target eccentricity (slope: 0.06 with 95% confidence range 0.045–0.074; Fisher’s  $r$  to  $z$ ,  $P<0.0001$ ), averaging  $1.1^\circ$  at  $4^\circ$  and  $1.9^\circ$  at  $20^\circ$  (insets in Fig. 2c, d, open rectangles; values for the two directions and the two target viewing modes lumped together). With \*/VOM, in contrast,  $s_{it}$  showed only a very weak increase with eccentricity (slope: 0.015 with 95% confidence range 0.009–0.021;  $P<0.0001$ ; insets in Fig. 2a, b;  $0.6^\circ$  at  $4^\circ$  and  $0.8^\circ$  at  $20^\circ$ ). Figure 2a also plots the indication SD for SSA from this and the following two series (asterisk), which marks the minimum  $s_{it}$  that can be achieved whatever the viewing condition.

The variability of indications across repeated trials (inter-trials SD  $s_{xt}$ ) is given by the filled triangles in the insets of Fig. 2. In contrast to  $s_{it}$ , it behaved fairly similar with all four viewing conditions ( $F=1.22$ ,  $P=0.32$ ). Similar as  $s_{it}$  with \*/RET probe viewing, it increased with target eccentricity, averaging  $1.3^\circ$  at  $4^\circ$  eccentricity and  $2.3^\circ$  at  $20^\circ$ .

### Visual-vestibular series (B)

In the visual-vestibular condition, the number of target eccentricities was reduced ( $0$ ,  $\pm 8^\circ$ ,  $\pm 16^\circ$ ) and the 12-s dark period between presentation and reproduction now con-

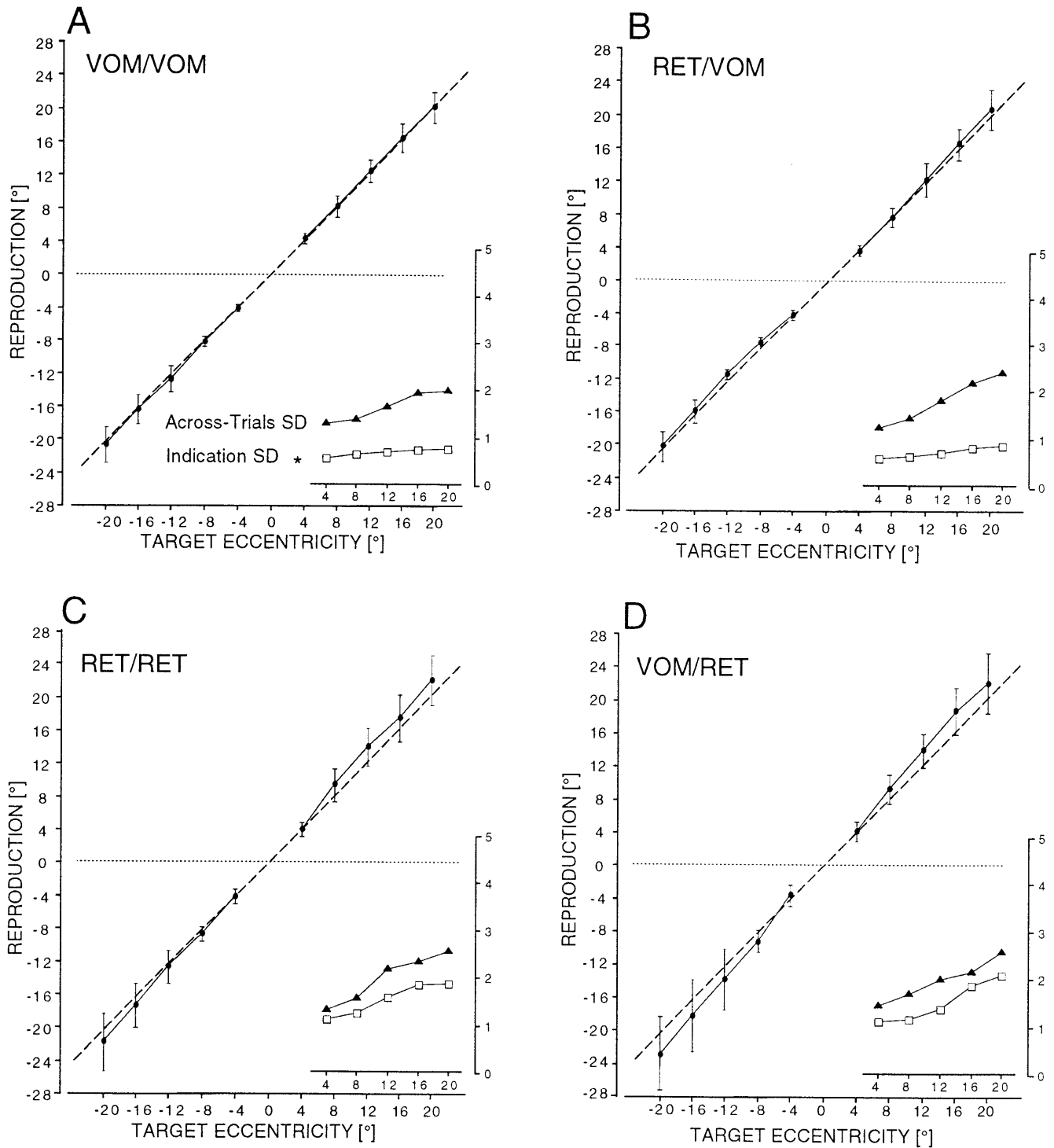


**Fig. 2a-d** Visual-only series. Reproduction of previously presented target location in space as a function of target eccentricity (positive values, to the right). Interconnected mean values (vertical bars,  $\pm$  SD means across-subjects variability). Dashed 45° lines give ideal performance. Insets show mean indication SD,  $s_{it}$  (open squares; asterisk,  $s_{it}$  of SSA) and across-trials SD,  $s_{xt}$  (solid triangles) as a function of normalised target eccentricity with respect to

SSA. The four viewing conditions are shown (compare Fig. 1, traces a-d): **a** VOM/VOM, **b** RET/VOM, **c** RET/RET, and **d** VOM/RET. Note that peripheral probe viewing reproduction (**c**, **d**) differs from foveal probe viewing reproduction (**a**, **b**) in that it yields higher values of indication SD, which furthermore clearly increase with eccentricity. Across-trials SD is similar in the four conditions

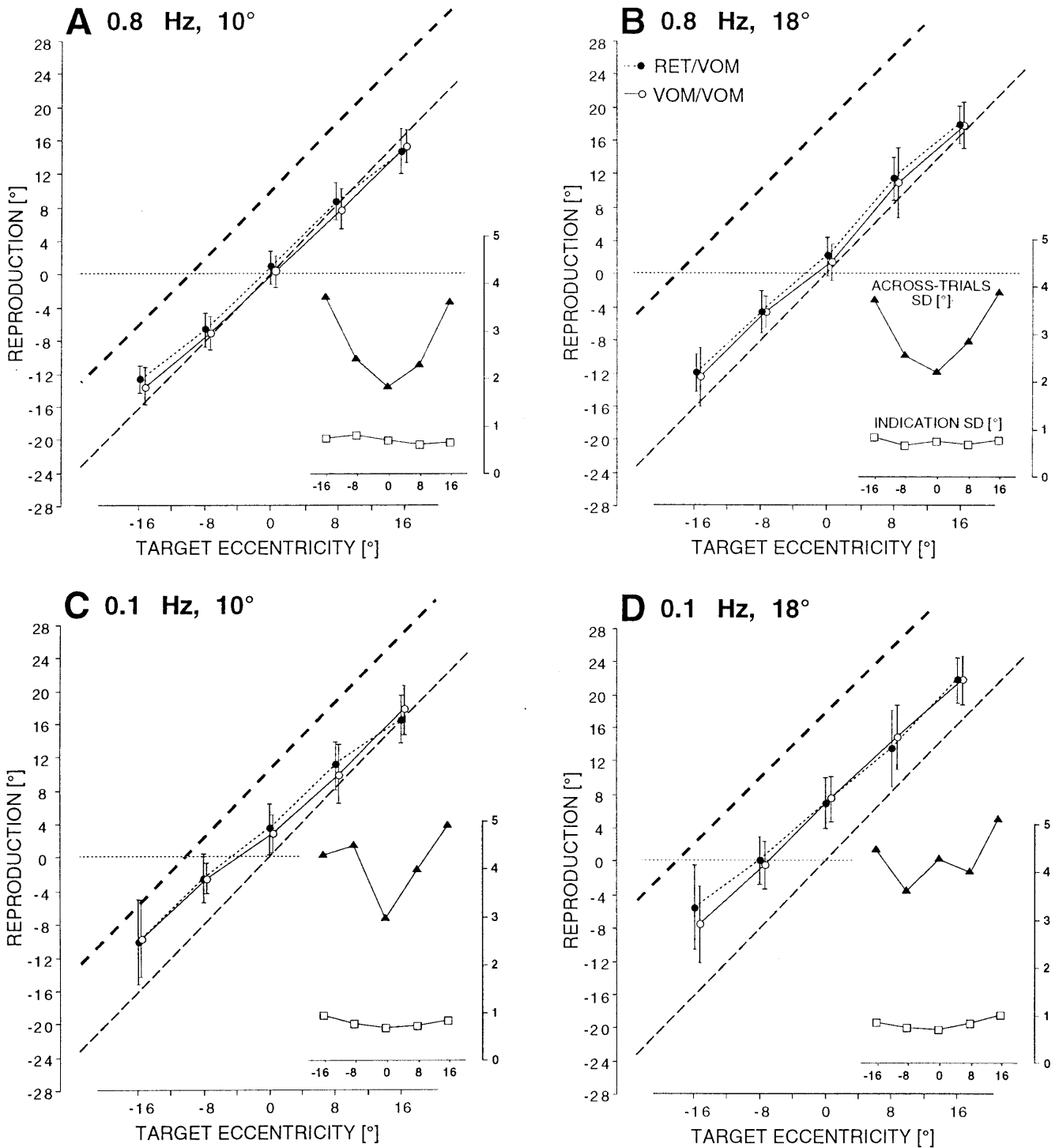


**Fig. 3a–d** Visual-vestibular series. The results for the four vestibular stimuli used: **a** 0.8 Hz, 10°; **b** 0.8 Hz, 18°; **c** 0.1 Hz, 10°; and **d** 0.1 Hz, 18° (dominant frequency, displacement). Mean reproduction values ( $\pm$  SD across subjects) as a function of target eccentricity (positive/negative values on *abscissas* here were obtained with body rotation towards/away from target). Data for viewing conditions VOM/VOM (open circles) and RET/VOM (solid circles) are superimposed. Thin dashed 45° lines, “ideal” performance; heavy dashed 45° lines, hypothetical performance of

subjects with absent vestibular function. The estimation curves for the 0.8 Hz (**a**, **b**) are close to ideal with both VOM/VOM and RET/VOM, whereas those for 0.1 Hz (**c**, **d**) are shifted towards the “no vestibular function” lines, indicating underestimation of body rotation. Furthermore, the slopes of the estimation curves are slightly below unity in **a** and **b**, and more so in **c** and **d**. Insets give means of indication SD (open squares) and across-trials SD (filled triangles) as a function of target eccentricity with respect to pre-rotatory SSA (0° on *abscissas*)

tained a body displacement. In order to keep the across-subjects SD low (compare visual-only series), only the VOM reproduction condition was retained. Mean SSA was again shifted slightly towards the right ( $2.0 \pm 2.8^\circ$ ) and also indication SD and across-trials SD of SSA were similar as before ( $\pm 0.55^\circ$  and  $\pm 1.8^\circ$ , respectively).

The estimation curves obtained after vestibular stimulation are shown in Fig. 3, separately for the two rotation frequencies (0.8 Hz and 0.1 Hz) and two amplitudes ( $10^\circ$  and  $18^\circ$ ). Different from the conventions of Fig. 2, the sign on the abscissas does not indicate absolute target eccentricity with respect to the initially adjusted SSA (right, left), but the relative direction of target eccentricity with respect to the direction of the subsequent body rotation (positive, same direction; negative, opposite). As a guide, thin dashed  $45^\circ$  lines show the response curves of an ideal observer, whereas the bold ones give the curves of an observer who does not sense body rotation (e.g. a patient with complete vestibular loss).

The two modes of target presentation (RET/VOM, Fig. 3, dotted curves; VOM/VOM, Fig. 3, continuous) yielded essentially similar results [repeated-measures ANOVA with factors Stimulus frequency (0.8 Hz, 0.1 Hz), Amplitude ( $10^\circ$ ,  $18^\circ$ ) and Target viewing mode (\*RET, \*/VOM);  $F=0.08$ ,  $P=0.78$ ]. The following description therefore refers to data pooled across both viewing conditions. For simplicity, consider first the localisation of targets presented at SSA (abscissa value,  $0^\circ$ ). Following the fast, brief rotations (0.8 Hz), subjects almost perfectly reproduced the target's spatial location. The intervening  $10^\circ$  ( $18^\circ$ ) angular displacement shifted their indication by only  $0.7^\circ$  ( $1.6^\circ$ ) in the direction of body rotation (upward with respect to the ideal lines in Fig. 3a, b), indicating that their vestibular compensation of the  $10^\circ$  displacement had a gain of 0.93 ( $G=(10-0.07)/10=0.93$ ; 0.91 in the case of  $18^\circ$  displacement). In contrast, with the slow, long-lasting rotations (0.1 Hz), the responses are shifted by a considerable amount towards the post-rotatory body position, with the corresponding gain values amounting to 0.64 (0.60) for the  $10^\circ$  ( $18^\circ$ ) body displacements.

Considering now also eccentric targets, we note that their localisation is affected by small (at 0.8 Hz) and large (at 0.1 Hz) shifts. Accordingly, the resulting estimation curves can be viewed as vertically shifted versions of the curves recorded before in stationary subjects (visual-only series), with the amount of the shifts being determined by the amplitude of body rotation and the vestibular gain. Noticeably, however, the slopes of these curves are no longer unity but smaller, averaging 0.92 at 0.8 Hz (95% confidence range, 0.83–1.01) and 0.83 at 0.1 Hz (0.70–0.95), with a tendency for lower values with the smaller amplitude of  $10^\circ$ .

Response indication SD  $s_{it}$  was similar to that in the visual-only series (open squares in insets of Fig. 3), apart from a slight, but statistically significant rise with 0.1 Hz as compared to 0.8 Hz ( $F=10.84$ ,  $P=0.001$ ). Across-trials SD  $s_{xt}$  (filled triangles) was clearly larger than in the visual-only series, with the largest values occurring at

0.1 Hz (difference across frequencies significant;  $F=16.67$ ,  $P=0.0009$ ), while rotation amplitude had no considerable effect. An observation of particular relevance is that at 0.8 Hz  $s_{xt}$  exhibits a *symmetrical* increase as a function of *spatial* target position (i.e. of pre-rotatory target-to-head eccentricity) with a corresponding minimum at SSA, irrespectively of whether after the rotation target-to-head eccentricity became small (ipsilateral rotation, positive abscissa values) or large (contralateral, negative). The corresponding data for 0.1 Hz do not contradict the notion of a SSA-centred symmetry of  $s_{xt}$ , because they are dominated by a conspicuous overall increase in noise. Finally, the vertical bars attached to the estimation curves in Figs. 2 and 3 indicate that also across-subjects SD is increased following the vestibular stimulus, and this more so with the 0.1-Hz as compared to the 0.8-Hz stimuli ( $F=6.92$ ,  $P=0.02$ ).

#### Visual-vestibular-neck series (C)

Only one viewing mode (VOM/VOM) and one rotation amplitude ( $18^\circ$ ) were used. However, the rotational stimuli now comprised, in addition to VEST, also NECK, VEST+NECK, and VEST-NECK (see Fig. 4c). Subjects' SSA was similar as in the previous two series (mean,  $1.14 \pm 2.45^\circ$ ;  $s_{it}$ ,  $0.55^\circ$ ;  $s_{xt}$ ,  $1.9^\circ$ ).

The reproduction curves are given in Fig. 4a, b (presentation as in Fig. 3; heavy dashed  $45^\circ$  line for observer with no body rotation sense only valid for VEST). For VEST (filled circles) similar curves were obtained as in the previous series, characterised by larger shifts towards post-rotatory body position with slow (Fig. 4b) as compared to fast rotations (Fig. 4a) and by slopes smaller than unity, again with a trend to decrease with frequency: 0.91 at 0.8 Hz, and 0.77 at 0.1 Hz.

The results for NECK (open circles) are plotted in an analogous way, except that the direction of the target now is referenced to the *relative* rotation of the head with respect to the trunk. Values on abscissas are positive when target eccentricity and head-on-trunk rotation have the same direction and are negative with the opposite direction. For instance, when head-on-trunk rotation is to the right (implying an actual trunk rotation to the left; compare Fig. 4c), target positions on the right of SSA are denoted by positive values. The indications of a (hypothetical) subject without a neck evoked rotation sense for trunk-in-space, indicating target-to-trunk instead of target-in-space position, would fall on a line shifted by  $-18^\circ$  on the ordinates (i.e. downwards; dotted heavy lines). Our subjects' estimation curve for the 0.8-Hz stimulus (Fig. 4a) is close to the ideal, falling only slightly below the  $45^\circ$  line (thin dashed), indicating a small shift in the direction of trunk displacement ("neck" gain,  $G=0.89$ ). However, its slope is again slightly below unity (0.91). The curve for 0.1 Hz (Fig. 4b) exhibits a large downward shift, indicating that subjects were centring their estimates almost about their trunk position ( $G=0.35$ ). The slope (0.86) again did not reach unity.

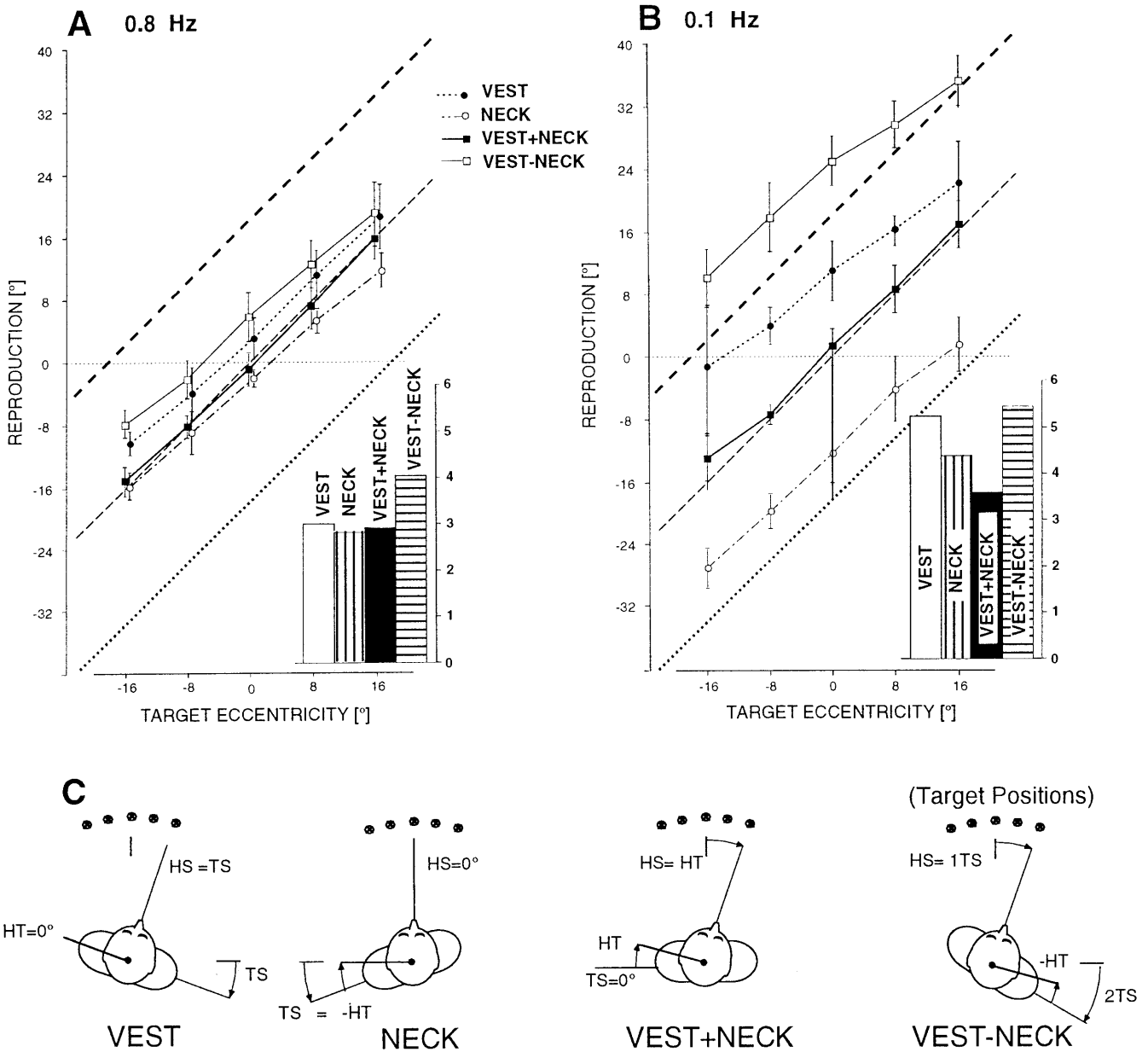


**Fig. 4a-c** Visual-vestibular-neck series (viewing condition, VOM/VOM). Superimposed in each panel are the results for the four stimulus combinations (compare c): VEST (*solid circles*), NECK (*open circles*), VEST + NECK (*solid squares*), and VEST-NECK (*open squares*). Presentation of estimation curves as in Fig. 3 (but “no vestibular function” *thick dashed lines* apply only to VEST; for details of direction normalisation with NECK, see text). **a** 0.8 Hz/18° stimuli; **b** 0.1 Hz/18° stimuli. Note that the estimation curves for VEST + NECK fall very close to the ideal 45° lines (*thin dashed lines*), both at 0.8 Hz and 0.1 Hz, while those for VEST-NECK show the largest offset from these lines. *Insets* give across-trials SD for the four stimulus combinations (averaged across all target eccentricities). **c** Pictographic representation of the four vestibular-neck stimulus combinations used (subject from above). [VEST whole-body rotation (head-in-space, HS, equals trunk-in-space, TS). NECK trunk rotation with head kept stationary (stimulus, head-to-trunk, HT). VEST+NECK head rotation on stationary trunk. VEST-NECK head and trunk rotation in space in same direction, but trunk with double amplitude]

Of particular interest are the curves obtained for head rotation on the stationary trunk (VEST+NECK; filled squares in Fig. 4). The curves fall almost exactly on the ideal 45° lines, irrespective of the frequency of rotation (hence a displacement gain at SSA of 0.99 at 0.8 Hz and of 0.94 at 0.1 Hz). The slopes are close to unity also (0.96 and 0.97, respectively). Thus, these estimations do not exhibit the frequency-dependent mislocalisations observed with all other stimulus combinations.

Finally, the estimation curves for VEST-NECK are given by the open squares in Fig. 4. The data are plotted in such a way that they were shifted by 18° (36°) in positive direction (upwards) if a subject reproduced the target’s position relative to the head (the trunk) instead of in space (compare Fig. 4c). Our subjects’ estimation curve for 0.8 Hz is not far from ideal; it is only slightly shifted upwards, but has a low slope of 0.86. On the oth-

er hand, a pronounced upward shift is seen for 0.1 Hz, combined with a decrease in slope (0.76), suggesting that the monomodal VEST and NECK mislocalisations at low frequency essentially add during this stimulus combination.

Indication SD  $s_{it}$  of reproduction was essentially similar to the previous series (range 0.79–1.05), showing only a slight increase with pre-rotatory target eccentricity, but no consistent dependency on post-rotatory head and trunk position (not shown). Across-trials SD  $s_{xt}$  exhibited no consistent relationship with target eccentricity and therefore was averaged across all eccentricities (bar graph insets in Fig. 4a, b). This mean depended on frequency ( $F=40.7$ ;  $P<0.0001$ ), being larger with low as compared to high frequency, as well as on stimulus combination ( $F=11.3$ ;  $P<0.0001$ ;  $2\times 4$  factorial ANOVA with factors Stimulus frequency and Stimulus combination). As to the stimulus combination effect,  $s_{xt}$  was always smaller during VEST+NECK as compared to VEST-NECK, and there was a significant interaction with frequency, in that VEST+NECK yielded significantly smaller values at 0.1 Hz than all other combinations (paired  $t$ -tests,  $P<0.03$ ). As before, across-subjects SD (SD bars attached to estimation curves in Fig. 4) was larger during slow than during fast rotations.

### Control experiments

A first control experiment tested the possibility that the reduced slopes of the estimation curves (values less than 1) observed in the previous two series owe to an interaction between (1) the eccentric presentation of a visual object (the target) in an otherwise dark room with (2) the evaluation of the subsequent rotational stimulus as a result of which SSA memory might undergo a shift. As in the previous experiments, subjects ( $n=3$ , 16 repetitions per trial) indicated SSA and tried to reproduce its location in space after the memory period. During the memory period, first a non-target visual stimulus was presented for 3 s at  $\pm 16^\circ$ , which subjects were to foveate. Immediately thereafter, subjects were rotated ( $\pm 18^\circ$ , 0.1 Hz) either towards the side of the meanwhile extinguished non-target (Same condition) or away from it (Opposite). Post-rotatory reproduction of the pre-rotatory SSA was erroneous, because of the underestimation of self-motion at 0.1 Hz. Interestingly, however, the error in the Same condition ( $-5.4$ , on average) was considerably less than in the Opposite condition ( $-9.0$ ; difference statistically significant,  $P<0.0015$ ). When the experiment was repeated without the intermittent vestibular stimulus, the effect of the non-target mostly disappeared ( $F=2.1$ ;  $P=0.11$ ).

A second control experiment investigated whether the minimum of  $s_{xt}$  is always centred at SSA (obtained with head and trunk aligned), as Figs. 3 and 4a, b would suggest, or whether it is linked to (pre-rotatory) head position. Therefore, the target was presented with subject's head laterally deviated by  $18^\circ$  (after an initial SSA indication as before and a subsequent 0.8 Hz VEST+NECK

stimulus in darkness to produce the head deviation). Target reproduction, in contrast, was performed after the head had been re-centred during the memory period (three subjects, target presented at  $0^\circ$ ,  $8^\circ$ ,  $16^\circ$  ipsilateral of the deviated head and at  $0^\circ$ ,  $8^\circ$ ,  $16^\circ$ ,  $24^\circ$ ,  $32^\circ$  contralateral; 16 trials per subject and target position). As in the previous experiments,  $s_{xt}$  reached a minimum at pre-rotatory SSA ( $2.2^\circ$ ) and increased with target eccentricity from SSA to either side (maximum of  $6.8^\circ$  at  $32^\circ$  contralateral).

---

## Discussion

### Mean accuracy of target localisation

#### *Effects of retinal and eye position signals*

In humans, the internal representation of a visual target's spatial location can only be assessed indirectly by inferences from behaviour. In the past, open loop manual pointing has been frequently used to this end (see Henriques et al. 1998; Lewald and Ehrenstein 2000). The results of these experiments revealed distortions related to how the target is viewed. With targets presented to the peripheral retina, there is a roughly constant pointing overshoot (about  $3^\circ$ ) in the direction of the target's retinal eccentricity (Bock 1986; Henriques et al. 1998; Lewald and Ehrenstein 2000). This "retinal magnification error" adds with a second error, related to orbital eye eccentricity, which causes a pointing deviation of about 12% counter to the direction of this eccentricity, resulting in an undershoot if an eccentric target is fixated during pointing (Lewald and Ehrenstein 2000).

No such errors were detected in the present experiments, which used an intra-sensory match-to-sample paradigm. It is true that our subjects' responses exhibited a slight overshoot with peripheral probe viewing (VOM/RET, RET/RET; Fig. 2). However, this small error is by no means compatible with the errors reported for hand pointing. For example, if there were a "retinal magnification error" of about  $3^\circ$ , a target presented at a retinal eccentricity of  $12^\circ$  (RET target presentation) would be registered in the memory with an eccentricity of  $15^\circ$ . Given, furthermore, an under-representation related to orbital eye eccentricity of 12% when the probe is fixated during reproduction (VOM), subjects would have to adjust an eccentricity of about  $17^\circ$  in order to match the probe with the  $15^\circ$  value stored in memory ( $16.8^\circ=15^\circ\times 1.12$ ). Clearly, the results obtained for RET/VOM do not exhibit the slightest trace of such an overshoot. By similar reasoning, an undershoot would result with the other crossed combination, VOM/RET, whereas the results in Fig. 2 show a reverse trend (a slight overshoot), at best. We therefore conclude that the reported manual pointing errors probably arise in the transformation of sensory information into the motor activity guiding the hand and that eye position is taken into account in an essentially ideal way for perceptual target

localisation as far as mean accuracy is concerned. Therefore, the analysis of mean accuracy tells little about the characteristics of internal target representation, in contrast to response variability.

### *Effects of vestibular and neck proprioceptive signals*

In series B and C, subjects underwent various combinations of body and/or head rotations. As long as these rotations were fast (0.8 Hz), subjects were able to maintain an almost correct notion of space so that the mean accuracy of their localisations was close to ideal. However, with 0.1-Hz rotations, two types of systematic mislocalisations were found in all situations (except with VEST+NECK) which we refer to as “trunkward shift” and “target eccentricity effect”.

*Trunkward shift.* Whenever the rotational stimuli included a displacement of trunk in space, the estimation curves were shifted away from their “ideal” course, in the direction of the trunk (compare stimulus pictograms in Fig. 4c with results in Fig. 4a, b), by an amount proportional to trunk rotation. These errors can be explained by noting that subjects can compensate for the intervening body (*en bloc* head and trunk) displacement only to the extent they *perceive* it. For VEST it is well known that slow rotations are underestimated, hence the incomplete compensation of the body rotation. Likewise, NECK stimulation has been shown to evoke a perception of trunk turning in space which decreases as rotation frequency is lowered, much as vestibular perception does; the direction of this turning perception obviously is in the direction of the actual trunk rotation and, hence, counter to that of the head relative to the trunk. Depending on the direction of the NECK and VEST stimuli relative to each other, the vestibular and neck-propriceptive underestimations of low-frequency rotations add together when the two stimuli are combined (which explains why errors are particularly large with VEST-NECK), or neutralise each other so that virtually no mislocalisation occurs with VEST+NECK (Mergner et al. 1991).

The observed trunkward shifts of target localisation and the above cursory explanation in terms of a linear summation fit well with a general view of human orientation in space which we have developed in the course of previous work and translated into a descriptive model. This model, which has been detailed elsewhere (Mergner and Rosemeier 1998; Mergner et al. 1997; compare also Mergner et al. 2000), will be considered later (Fig. 6a, box “Vestibular-neck interaction”, explained in Appendix B). Briefly, we have suggested that humans tend to equate “space” to their visual, auditory and haptic environment as long as this environment, and in particular the body support, is stationary. Stationariness of the support (generally, its kinematic state) is monitored by afferents from the vestibular sensors, after appropriate compensation for trunk and head movements *relative* to the support. This compensation is based on the principle

that, as long as vestibular activity can be accounted for by such relative movements, the support must be stationary; otherwise, it is interpreted as support motion in space (at least in the absence of other external references; see also Appendix B). A detected support motion acts as a “dynamic space signal” from which the support’s current displacement relative to a previously established “static space reference” can be derived. Knowing this displacement, and the body’s torsional movements about his/her point of abutment from proprioceptive afferents, the subject can relate current head displacement and eye displacement to the static reference (“absolute space”), irrespective of whether these displacements result from support motion or from propiersonal motion about the support. The model derived from these ideas generates close-to-reality predictions regarding the perceptions of head-in-space, trunk-in-space and head-on-trunk rotation that result from arbitrary combinations of VEST and NECK stimuli over a large range of frequencies (Mergner et al. 1991). With appropriate additions for (1) the retinal and oculomotor contributions to target localisation and (2) the inscription into, and retrieval from the memory, it also predicts the present data (Appendix B and Fig. 6b).

Expanded in this way, the model describes perceptual target localisation in space as relying on two sets of coordinate transformations. One set of transformations serves to sense the kinematic state of the body support in the way sketched above and, therefore, to derive current head displacement relative to the static space reference. Using this head displacement signal, the second set changes the representation of both the target and the probe from eye-centred into space-referenced. Taken together, these transformations can be viewed as reversing the physical transformations of the target (probe)-to-eye position occurring during eye, head and trunk movements. As a result, at the level of the memory and the probe-to-memory matching, target and probe positions are “clamped” to reflect the initial (pre-rotatory) state, irrespective of intervening eye, head and trunk rotations – with the notable exception of slow trunk rotations which, because of the imperfect performance of the vestibular system, lead to the observed trunkward shifts.

To appreciate the explanatory power of the model, consider why slow trunk rotations about the stationary head (NECK, 0.1 Hz) also cause trunkward shifts. According to the vestibular-neck interaction part of the model, such movements cause an illusory perception of head deviation in space counter to the trunk rotation (compare Mergner et al. 1991), hence a corresponding shift of apparent probe position along with the head. To match the probe with the remembered target position, the subject must offset this illusory displacement of the probe, by shifting it in the direction of trunk rotation.

There are other schemes that also could explain the observed localisation performance. For example, with each detected head rotation, the memory could be reorganised (updated) so as to reflect target position relative to current gaze direction. The reason why we have sug-

gested the arrangement in Fig. 6a, where the memory contents remains “frozen” during the memory period and where its matching with probe position thereafter depends on the updated internal notion of current eye position relative to SSA, will become clear in Response variability.

Finally, as to the internal transformations, we point out that only for co-axial rotations can the hypothesised transformations be represented by simple summing junctions. In a more general situation non-linear operations are required. Therefore, the operations postulated by our model are unlikely to be carried out in terms of uniquely identifiable “analogue” signals (such as the frequency and recruitment coded signal of eye position in the oculomotor nuclei). Rather, they may result from the interaction of non-linear, position coding representations on two-dimensional (or multi-dimensional) neural maps (compare Pouget and Snyder 2000). Possible examples of this type of neural computation have been observed by Andersen et al. (1985).

*Target eccentricity effect.* Whenever there was a trunk rotation, the estimation curves not only were shifted with respect to the veridical curves, but also exhibited a slope of less than unity. Again, this effect was larger at the low than at the high frequency. With VEST+NECK, where the trunk was stationary, no such slope reduction occurred. Our control experiment with SSA reproduction following the presentation of a non-target eccentric visual stimulus suggested that it reflects a shift of the post-rotatory estimate of SSA, associated with trunk rotation if this rotation was preceded by an eccentric visual stimulus.

We have implemented this suggestion in our model by assuming that target eccentricity exerts a bias which increases sensed trunk-in-space rotation, in proportion to target eccentricity, for ipsilateral rotation (with respect to the target) and decreases it for contralateral rotation. When we added such a bias to our model (dotted in Fig. 6a), sensed trunk rotation and reproduced target position became modulated in a way similar to the experimental results: the slope of the simulated estimation curves (Fig. 6b) decreased slightly at 0.8 Hz and markedly at 0.1 Hz, except for VEST+NECK, where it retained its unity value (a relevant factor for this particular behaviour during isolated head rotation is the sensory threshold contained in the vestibular-neck interaction part of the model; see Appendix B).

The hypothesised bias is possibly related to earlier observations that SSA can be modified visually. For instance, anisotropies of visual space such as a luminance difference between right and left (e.g. a single, eccentric light spot as in the present experiments) can bias SSA (see Howard 1982). A detailed explanation for the result of our control experiment is still lacking, though (bias almost absent without trunk rotation and clearly present after intervening trunk rotation).

There are recent observations by Blouin et al. (1997, 1998a) of a non-linear visual-vestibular interaction dur-

ing updating of visual target location in space, which the authors attribute to a *general* underestimation of vestibular self-motion perception occurring in association with pre-rotatory target eccentricity. We find it difficult to integrate this notion into the hypothesised framework discussed here; attempts to have our model reproduce their findings failed.

## Response variability

### *Effect of viewing conditions*

As a major result of series A, we recall that the mode of target viewing (VOM/\* or RET/\*) was essentially irrelevant for both indication ( $s_{it}$ ) and across-trial ( $s_{xt}$ ) variability. In contrast, the mode of probe viewing (\*VOM or \*/RET) clearly had differential effects (cf. synopsis of SD curves from Fig. 2 in Fig. 5a, b): while the across-trials variability  $s_{xt}$  increased as a function of target eccentricity whatever the mode of probe viewing (Fig. 5b), the indication variability  $s_{it}$  exhibited such an increase only with \*/RET and was almost independent of eccentricity with \*/VOM (a). What can we learn from these two variability measures?

The *indication SD*  $s_{it}$  reflects variations of (1) the internal signal coding probe position and (2) the memory trace during the period of probe-to-memory matching. We assume that the variability of the memory trace in one and the same indication sequence is small and, hence, that  $s_{it}$  mainly is determined by the variability of the probe position signal. The latter draws on two sources, one related to retinal probe eccentricity, the other one to orbital eye position. The eccentricity-dependent increase in  $s_{it}$  for \*/RET probe viewing conceivably is caused by an anisotropic spatial resolution of the signal reflecting the probe’s “*absolute*” location on the retina and its representations in the CNS (paralleling, but not equalling, the anisotropy of visual acuity which shows a much finer resolution, because it reflects a *relative* measure between at least two visible objects). For \*/VOM (probe at fovea),  $s_{it}$  reaches a minimum which, we suggest, mainly reflects the variability of the *eye position* signal. In its purest form its variability is given by the  $s_{it}$  values obtained during SSA indication (about  $0.6^\circ$ ). This value, but also those observed during VOM reproduction ( $0.6$ – $0.8^\circ$ ), is compatible with the data of Karn et al. (1997), who derived an upper limit of  $1.4^\circ$  from an investigation of memory-guided saccades.

The *across-trials SD*  $s_{xt}$  draws on at least three different noise sources, corresponding to a dissection of the experimental task into three main processes: (1) localisation of the target, (2) storage and maintenance in memory, and (3) localisation and matching of the probe (the latter being essentially reflected by  $s_{it}$  considered here). As detailed in Appendix A, the contribution from  $s_{it}$  can be removed by appropriate calculations. The result of this calculation, shown in Fig. 5c, indicates that the compound variability representing the noise associated with

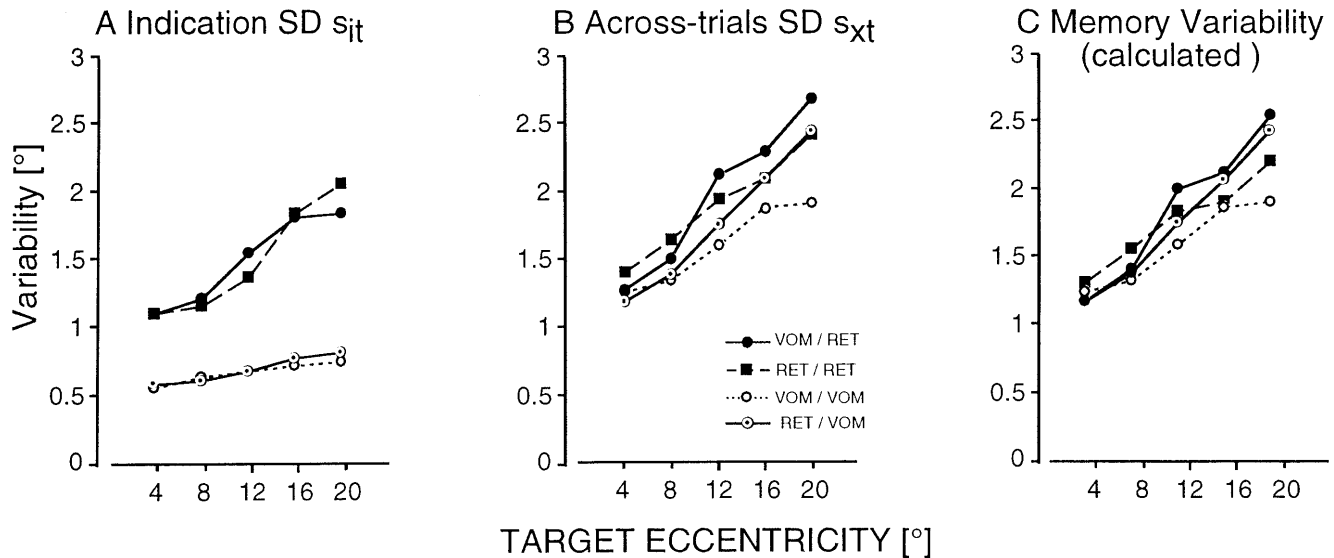


**Fig. 5a–c** Superimposed variability data from visual-only series (indication SD in **a**, and across-trials SD in **b**), taken from Fig. 2, for comparison with the calculated memory variability (**c**). Mean variability curves for the four viewing condition used are plotted as a function of normalised target eccentricity with respect to SSA. Note that across-trials SD is essentially independent of viewing condition. Memory variability is similar to across-trials SD

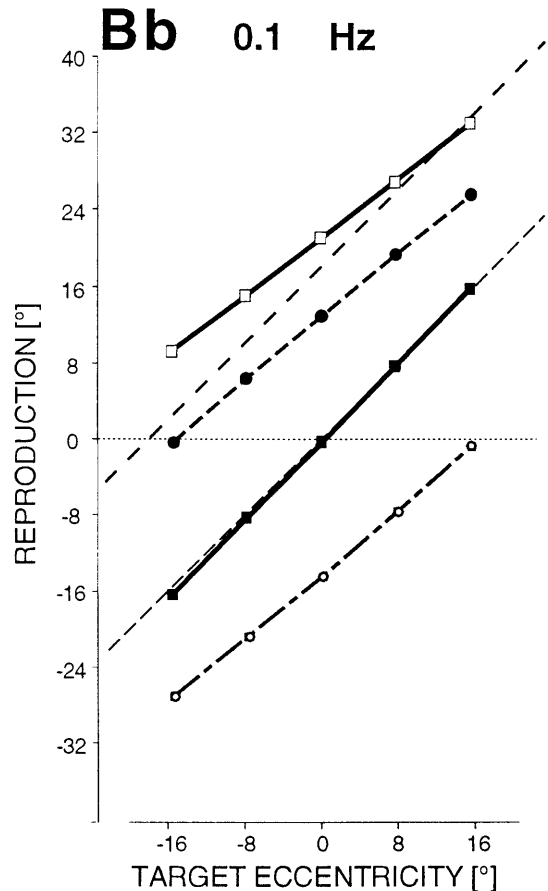
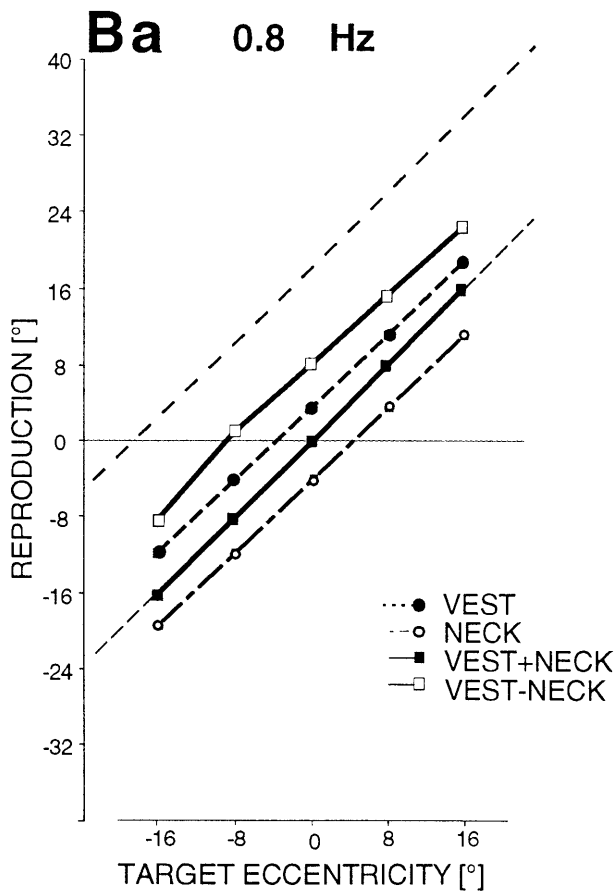
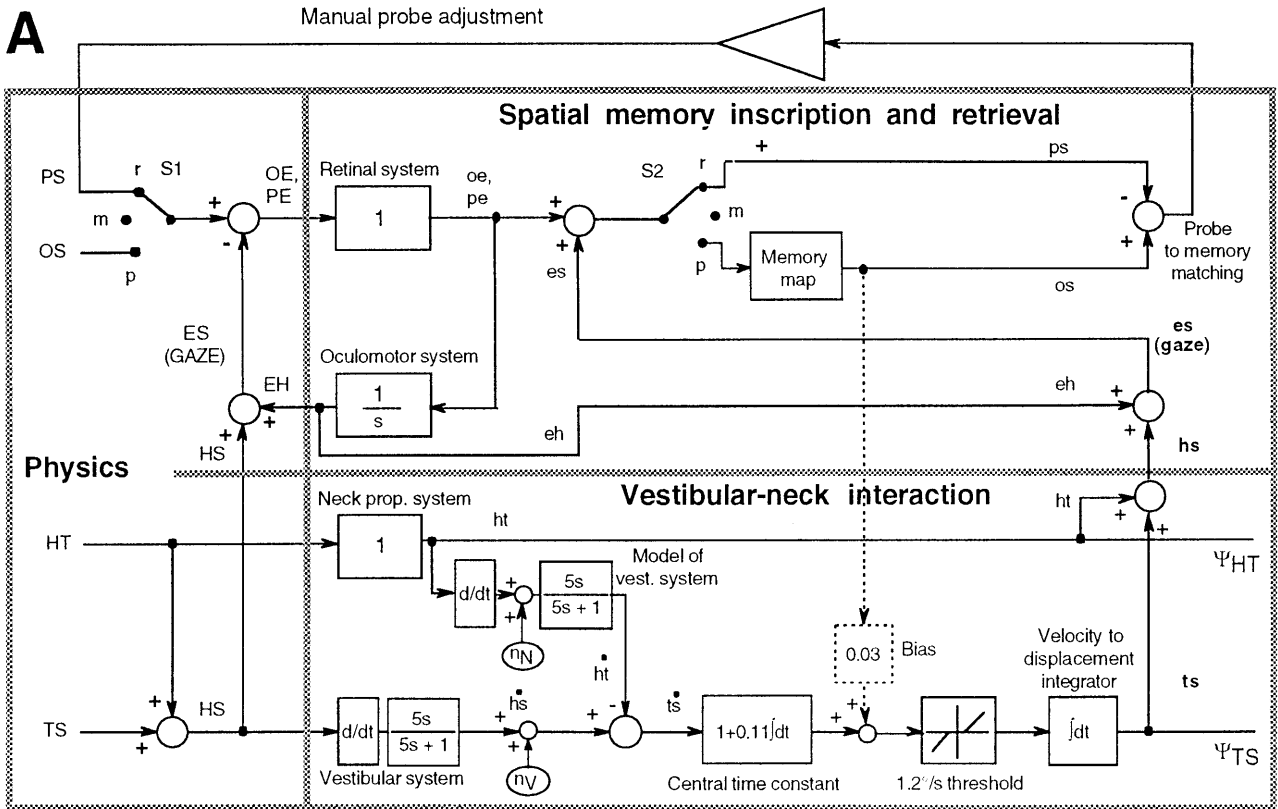
processes 1 and 2 is remarkably similar in all four viewing conditions. We argue (Appendix A) that the noise from the target localisation process can largely be neglected, or merged with that of the memory trace, since  $s_{xt}$  is essentially independent of the mode of target viewing. In other words, we suggest that the calculated variability curves in Fig. 5c mainly represent the variability of the memory trace across the whole memory period. We refer to it as “memory variability”.

An outstanding property of this memory variability is its increase with target eccentricity relative to SSA. This property suggests that the target location is stored in a memory map whose angular resolution decreases with eccentricity, giving its noise a “retinal character”. Moreover, the similarity of this anisotropy across all four viewing combinations (Fig. 5c) suggests that the memory trace is, by and large, independent of the mode of target viewing. In other words, whether subjects look straight ahead during target presentation or whether they gaze at the target, target location apparently is stored on a map which always remains aligned with the notion of “space” acquired prior to the memory period (SSA in primary head-on-trunk position). Remarkably, the same appears to be true for situations in which the head is deviated during target presentation, as suggested by our second control experiment. The occurrence of an anisotropy as such, and its centring on SSA during RET viewing, are acceptable facts in view of the increasingly coarser “grain” towards the periphery of the retina and its representation in V1 and higher visual areas, and is also observed with measurements of *absolute* localisa-

tion thresholds (White et al. 1992). However, the continuing alignment with SSA even when an eccentric target is foveated could not be readily predicted.

Even more surprising is the finding that the alignment with SSA appears to continue across intervening body rotations; this conclusion is suggested by the symmetry of the  $s_{xt}$  curves obtained in the vestibular stimulation series at 0.8 Hz (Fig. 3), which indicates that  $s_{xt}$  continues to depend only on target eccentricity with respect to pre-rotatory SSA, regardless of whether the body subsequently is rotated towards or away from the target, and that it always reaches a minimum at SSA. It is this firm alignment of the point of minimal across-trials variability with SSA which led us to suggest that the inscription into, and the read-out from, the memory occurs always in terms of spatial coordinates, as sketched in Fig. 6a. The particular mechanisms which could ensure this coding scheme have been discussed above (internal inversion of external physical coordinate transformations of current gaze axis with respect to pre-rotatory SSA).

The notion of the representation of target position referring to a fixed position in space may appear counter-intuitive at times, because it is a frequent introspective experience that space and target appear to move “before the inner eyes”, counter to the self-rotation. It is tempting to interpret this experience as reflecting an *updating* of the spatial memory map in egocentric coordinates, in conflict with the notion of a “frozen” one. However, when asked to specifically report experienced motion of the target *in space*, subjects considered target and space as stationary and the self as moving. Thus, introspective experience depends on whether attention is directed at events in the egocentric or the space-centric reference frame. When “space” is attended, it is the perceived current body position which is updated by referencing it to its pre-rotatory position, that is, to pre-rotatory SSA. Conceivably, this is different in hand-pointing tasks where the moving arm segments are anchored on the body and therefore might be referenced to the trunk. Possibly, the trunk-centric and space-centric references are



interchangeable (assuming that the brain has found ways to overcome, or to avoid the problem of non-commutativity of rotation angles with complex, non-coplanar rotations), with the choice of the reference depending on the task and the focus of attention.

Why would it be advantageous to maintain the memory trace in a fixed alignment, instead of realigning it with gaze after each eye and/or head movement? With the latter scenario, eye movements occurring during the memory period would repeatedly shuffle the memory trace back and forth between areas of high and low resolution on the map, thus causing an accumulation of errors. Such a scenario is very unlikely, however, to judge from the precision of returning to a previously assumed eye position after many (30) intervening saccades as observed by Skavenski and Steinman (1970). From their data, an across-trials SD of  $0.8^\circ$  is calculated, a figure which leaves little room for accumulated errors (true also for our localisation task when we extended the memory period to 40 s in pilot experiments). It is true that others (Karn et al. 1997) have observed some deterioration of the accuracy of memory-guided saccades with intervening eye movements. Yet, based on a comparison of (1) the added variance per intervening saccade and (2) the variability of visually guided saccades, Karn et al. (1997) felt that this effect owes to a non-specific interference with spatial memory. Rather they concur with the conclusion reached above that remembered targets are held in a head-centred frame of reference (“space”, since the head remained stationary in their experiment). Apparently the mechanisms of target re-localisation also take into account involuntary eye movements like those elicited by the vestibulo- and cervico-ocular reflexes; in a previous, related study with saccadic eye pointing, we compared target reproduction after body rotation with and without a head-fixed fixation spot (used to suppress these reflexes) and found no considerable difference (see Mergner et al. 1998).

Against our notion of a fixed, space-referenced representation of the target’s position in memory, one might object that the large majority of electrophysiological data gathered in various cortical and subcortical areas during attentional and eye movement tasks indicates a predominance of retinotopic representations, while neuronal pop-

ulations with head-centric receptive fields have only rarely been encountered as yet (see Moshovakis and Highstein 1994; Schall 1995). However, in principle at least, eye movement/position-dependent modifications of the primordial retinal representation are biologically feasible, as demonstrated for saccade-related neurons in the parietal cortex (Andersen et al. 1990; in terms of a population coding) and cortical visual neurones (Bremmer 2000), for instance.

So far we had made no attempts to establish in detail the relationship between memory variability and the duration of the memory period, which had a fixed value of 12 s in the present experiments. Observations by White et al. (1994) on memory-guided saccades in monkey suggest that variability increases rapidly at the transition from a visually linked to a memory-linked representation occurring during the first 0.8–1 s following the presentation of the target, but remains relatively stable thereafter (compare our 40-s memory period). Similar detailed work in humans so far has been restricted to memory periods not exceeding 1.6 s (White et al. 1992) and does not allow an extrapolation to the 12 s used here.

Finally, looking for alternative explanations of the observations made in the present experiments, one might ask whether subjects possibly could have remembered a certain pattern of oculomotor effort or of joystick excursion. This is unlikely, however, because the only condition which would allow an oculomotor effort-matching, VOM/VOM, did not differ from RET/VOM; and the second possibility can be excluded also, because the random target steps occurring during the indication sequence uncoupled joystick position from target position.

#### *Contribution of vestibular signal to response variability*

Although vestibular stimulation did not disrupt the symmetry of the relationship between  $s_{xt}$  and target eccentricity, it considerably raised the noise level as a whole, in particular at the low rotational frequency (0.1 Hz). Similar observations were made with neck stimulation. These results could be predicted from previous work (Mergner et al. 1991), which suggested that the central processing of the vestibular signal inevitably increases the variability of the internal estimate of head displacement in space, and this the more so the lower the frequency. In order to compare in more detail the present results with the prediction of the vestibular-neck interaction mechanism sketched in Fig. 6a, we pooled the figures of  $s_{xt}$  for all target eccentricities and compared the resulting global figure across stimulus conditions (bar graphs in Fig. 4).

The most illuminating finding is that, in the case of slow rotations, variability was lowest in the head-only condition (VEST+NECK), that is, in just that condition for which the interaction of vestibular and neck afferents appears to be optimised according to our model (recall that VEST+NECK caused no shift of the reproduction

◀ **Fig. 6** **a** Model of vestibular-neck interaction and of the contribution this interaction makes to the reproduction of target position in space after head-to-trunk (HT), trunk-in-space (TS) and head-in-space (HS) displacements. **b** Model simulations of the visual-vestibular-neck series (compare Fig. 4). For details, see Appendix B. Abbreviations *ht*, *ts* and *hs* give internal representations of HT, TS and HS, respectively (a *dot on top* indicates first derivative, i.e. the corresponding velocity signal; the addition of  $\psi$  denotes the self-motion perception derived thereof). *ps*, *os*, *eh* and *es* give the internal representations of probe-in-space, object-in-space, eye-to-head and eye-in-space displacements (*PS*, *OS*, *EH*, *ES*), respectively. The switches *S1* and *S2* can be closed during object presentation (position *p*) or reproduction (*r*) and are open during the memory period (*m*).  $n_V$  and  $n_N$  give sources of white noise injected into the vestibular and dynamic neck proprioceptive channels, respectively

curve; see also Appendix B). Using Monte Carlo simulations of the effect of noise in the vestibular and neck sensory channels on perceived trunk-in-space perception, we were able to show that this low variability with VEST+NECK does occur also in our model and is, in fact, a consequence of its optimisation for the case of pure head movements (Appendix B). Our simulations also indicate that little differences between conditions can be expected with fast rotations (0.8 Hz), in good agreement with most of our experimental findings (Fig. 4a). An exception is the fast VEST-NECK condition, in which  $s_{xt}$  is larger than in all other conditions. Possibly, this combination is experienced by subjects as a distinctly unusual situation and therefore receives additional variability of cognitive origin.

In a previous study, Blouin et al. (1998b) have reported minimal reproduction variability in a similar task with isolated head (VEST+NECK) or trunk rotation (NECK) as compared to combined head and trunk rotation (VEST), which at first glance appears to be in agreement with our findings at 0.1 Hz. Yet, their results are at variance with ours, in that they all were obtained with short-lasting rotations equivalent to about 1 Hz. Our findings and simulations at 0.8 Hz revealed no considerable difference in reproduction variability across these stimuli. Possibly, the rotational stimuli used by these authors contained low-frequency components, since they were performed manually. Furthermore, in the NECK situation, their subjects could use an external reference, since their heads were knowingly fixed with respect to a ground-based support, unlike with VEST.

## General conclusions

Our findings suggest that subjects who recall the location of a previously seen visual target in space after intervening eye, head and trunk movements are resorting to a “snapshot” of the target’s position in space taken prior to the movements, which is stored in a spatial memory map. Basic characteristics of this map are:

- a) It shows an anisotropic resolution of “retinal” character with low noise (high resolution) for targets close to SSA and larger noise (lower resolution) for eccentric targets. The alignment with pre-rotatory SSA is maintained irrespective of intervening eye, head and trunk rotations (“frozen map”).
- b) During reproduction, the probe’s position is back-transformed into pre-rotatory SSA coordinates (i.e. space) by reversing the physical transformations resulting from the eye, head and trunk rotations that have occurred during the memory period. Back transformation is based on efference copy (e.g. eye position) and sensory signals (retinal eccentricity, vestibular and neck afferents).
- c) Back transformation is correct only to the extent that the vestibular afferents veridically reflect head rotation. At low frequencies reproduction becomes erro-

neous, therefore. The observed errors are compatible with an earlier model according to which head-in-space position is only indirectly derived from the vestibular afferent signal, by first having this signal interact with a neck afferent signal to estimate the kinematic state of the trunk and its support; summation with a second neck signal then yields the estimate of head in space displacement which contributes to transform retinal probe position back into pre-rotatory SSA coordinates.

In a broader sense, these interpretations of the present experimental results reflect the view that, in the absence of visual and auditory orientation cues, the contact made by the body with its support constitutes an “interface” between the self and perceptual space. This view comes close to the “Standpunkt” coordinate concept of Müller (1916). This author extended earlier concepts of the egocentric reference systems of Hering and Helmholtz, by postulating separate gaze, head and standpoint reference systems. He reported observations he himself, or his subjects made when storing in memory the spatial geometry of a visual object for given orientations of gaze, head and trunk and recalling the geometry after having changed these orientations. He found that the geometry could then be conservative with respect to either gaze, head or standpoint, with the latter prevailing.

**Acknowledgements** Supported by DFG, Me 715/4-3 and Be 783/3. We thank W. Krause for his technical assistance and Dipl.Ing. T. Boß for designing and carrying out the Monte Carlo simulations.

## Appendix A

### Decomposition of across-trials variability

The three consecutive processes into which the subject’s task can be decomposed (spatial localisation of target, inscribing and maintaining a memory trace, and localisation of probe and matching to memory trace) are viewed as separate, *independent* sources of noise with Gaussian distribution. The possibility of correlated errors, e.g. in the wake of variations of vigilance, is neglected here. Characterising these sources by their SDs  $s_1$ ,  $s_2$ , and  $s_3$ , respectively, total variability can be expressed by  $s_{tot} = \sqrt{(s_1^2 + s_2^2 + s_3^2)}$ . Because the contribution of  $s_3$  was reduced by averaging across 4 repetitions of the matching procedure, the calculated across-trials variability  $s_{xt}$  is slightly smaller:

$$s_{xt} = \sqrt{(s_1^2 + s_2^2 + s_3^2/4)} \quad (A1)$$

The indication SD  $s_{it}$  is an estimate of  $s_3$ ; the finding that  $s_{it}$  is almost independent of target eccentricity for \*/VOM, but rises with eccentricity for \*/RET, is compatible with the notion that the central representation of the probe bears “retinal” noise characteristics related to the probe’s current retinal eccentricity.

For the other two components of  $s_{xt}$  ( $s_1, s_2$ ) our data provide no *direct* estimates. However, with regard to  $s_1$ , which arises during target localisation, it is fair to assume that it shows a similar dependency on retinal eccentricity to  $s_3$ . With this in mind, we now can try to infer the characteristics of  $s_2$  (*memory variability*), considering the following two straight-forward hypotheses:

- I. Memory variability  $s_2$  is much smaller than target localisation variability  $s_1$ . If so,  $s_{xt} \approx \sqrt{(s_1^2 + s_2^2/4)}$ . Hence  $s_{xt}$  would qualitatively exhibit the same behaviour as  $s_3$  and  $s_1$ , i.e. only a weak dependency on target eccentricity during VOM/VOM, but a clear rise during RET/RET. This hypothesis is contradicted by our experimental observation that  $s_{xt}$  exhibits a very similar increase with target eccentricity in both the VOM/VOM and RET/RET viewing conditions (Fig. 5b).
- II. Memory variability  $s_2$  is substantially larger than  $s_1$ . If so, then  $s_{xt} \approx \sqrt{(s_2^2 + s_3^2/4)}$  or  $s_2 \approx \sqrt{(s_{xt}^2 - s_3^2/4)}$ . Eliminating probe variability  $s_3$  by solving Eq. A1 yields the memory variability curves shown in Fig. 5c. These curves differ only slightly among the various viewing conditions and closely resemble the across-trials SD curves in Fig. 4b (because of the small effect of  $s_3^2/4$ ).

We therefore give credit to hypothesis II, holding that the across-trials SD curves in Figs. 2 and 3a, b essentially reflect the noise on the supposed memory map and its increase with spatial eccentricity (the across-trial SD curves in Figs. 3c, d and 4 are considered in Appendix B).

## Appendix B

### Model of vestibular-neck interaction and reproduction of spatial target position

The block labelled “Vestibular-neck interaction” in Fig. 6a describes how the interaction of vestibular and neck afferents determines the perceptions of self-rotation (for details, see Mergner et al. 1991). After a brief outline of the model, we will use it as a framework to discuss the trunkward shift, the target eccentricity effect, and the dependence of across-trials SD on VEST and NECK stimulus combinations (“vestibular noise”).

#### Model

The model of vestibular-neck interaction rests on the following key ideas:

1. The vestibular horizontal canal system delivers a signal of head-in-space velocity ( $\dot{h}s$ ). This signal is ambiguous in the sense that it can arise from a rotation of the subject as a whole (e.g. on a rotation chair) or from a rotation of the head on the trunk. The model disambiguates  $\dot{h}s$ , by determining to which degree it

can be explained by a head-versus-trunk rotation (HT). To this end, a version of the neck afferent signal is fed through an *Eigen-model* of the vestibular signal’s pathway, resulting in a signal of angular head-on-trunk velocity ( $\dot{h}t$ ) having the same transfer characteristics as  $\dot{h}s$  (i.e. the 5-s peripheral vestibular time constant). During any kind of head rotation (slow or fast) on the stationary trunk (VEST+NECK),  $\dot{h}t$  always equals  $\dot{h}s$ , hence  $\dot{t}s=0$ , indicating trunk stationarity. Thus, the system is optimised for the VEST+NECK case, in that  $\dot{t}s$  gives a veridical description of the state of the trunk in this case, regardless of the particular pattern of head movement. In other conditions, e.g. when the trunk is rotated together with the head (VEST) or about the stationary head (NECK),  $\dot{t}s$  is affected by the system’s time constant. For instance, it will underestimate actual velocity, or even become zero, when trunk rotation is slow.

2. The time constant of vestibular perceptions and of vestibularly based behaviour (15–20 s) is clearly longer than the 5 s of the peripheral organ. Accordingly, the model assumes a central “improvement” of the vestibular time constant by partial integration of the raw velocity signal  $\dot{t}s$  (term  $0.11 \int dt$  in Fig. 6a). However, this improvement has the negative side-effect of amplifying any low-frequency noise present in the peripheral vestibular signal. This noise would cause large errors upon conversion into a signal of angular displacement in the ensuing velocity-to-displacement integrator. To prevent such errors, this integrator is shielded by a  $1.2^\circ/s$  threshold (value determined experimentally; Mergner et al. 1991) that effectively blocks the noise as long as there is no supra-threshold  $\dot{t}s$  signal – as is the case during head rotation on the stationary trunk (VEST+NECK). In contrast, when the signal of estimated trunk-in-space velocity ( $\dot{t}s$ ) exceeds  $1.2^\circ/s$ , the noise that rides on top of it will be carried across the threshold.
3. The estimate of angular trunk displacement in space ( $ts$ ), derived by integration of  $\dot{t}s$ , is also a perception of support rotation in conditions where the feet are in fixed alignment with the support. It constitutes the basis for the perceptions of head-in-space displacement ( $hs$ ) by summation with a “tonic” neck signal ( $ht$ ), which shows essentially ideal transfer characteristics. Therefore, it depends on  $ts$  whether the perception mediated by  $hs$  is veridical or erroneous.

For the purpose of interpreting the present results two additional sections were added to the model:

1. The block “Physics” represents the target’s (here called object) and the probe’s positions in space (OS and PS, respectively) as well as the transformation of these positions from spatial into retinal coordinates (object/probe-to-eye signal, OE/PE) by ES, the current gaze position (eye-in-space), which is the sum of EH (eye-in-head position) and HS (head-in-space).

2. Box “Spatial memory inscription and retrieval” represents the internal processing of the resultant retinal signals (oe; pe) and the processes of inscription into the memory and probe-to-memory matching. Processing of oe (or pe) essentially consists of a back-transformation of this signal into space coordinates by means of an internal representation of gaze position (es), derived from internal representations of eye-in-head (eh; efference copy) and hs (provided by the vestibular-neck interaction section). The oculomotor system, shown as an integrating controller (1/s), is active if subjects fixate at the target (or probe). Its dynamics are not addressed here.

*Model simulations* started from an initial state (SSA) in which trunk, head and eyes were aligned in space (i.e. with SSA). During the *presentation* of the object (switches S1 and S2 in position  $p$ ), we therefore have  $ts=0^\circ$ . Furthermore, because the effects of eye and head (gaze) movements are neutralised by the internal gaze signal es, the signal of object in space inscribed into memory is identical to the object-to-trunk eccentricity at the outset of the memory period ( $os=ot$ ) and to retinal eccentricity in case of straight-ahead gazing.

During the *memory period* (switch positions  $m$ ) TS and HT signals (reflecting the stimulus under consideration) were applied, and the gain of ts was adjusted to be slightly smaller than unity (0.9). During *reproduction* (switch positions  $r$ ) the difference between the internal representation of the probe position ps (after back transformation into spatial coordinates by es) and the memory content drives the physical probe position PS until this difference becomes zero; PS then is noted as the model’s reproduction response.

### Trunkward shift

The shifts of the estimation curves in the direction of trunk rotation reflects the degree to which estimated and actual trunk (= support) displacement differ. Indeed, given that eh, ht, and os are veridical and that ps exactly is matched to os, the following relation holds:

$$ps=PS-ES+eh+ht+ts=os \quad (B1)$$

noting that  $ES=EH+HT+TS$ ,  $eh=EH$  and  $ht=HT$ , the above relation can be rewritten as:

$$PS=os+(TS-ts) \quad (B2)$$

thus confirming that the probe always will be shifted in the direction of TS, by an amount equalling the difference between actual (TS) and sensed (ts) trunk rotation. This difference increases when the dominant frequency of TS is lowered.

### Target eccentricity effect

The reduced slopes of the reproduction curves with TS is explained by a cross-coupling that biases  $\dot{ts}$  in the direc-

tion of os (dotted line in Fig. 6a). This bias cannot cross the  $1.2^\circ/s$  threshold as long as  $\dot{ts}$  otherwise is zero; thus it cannot affect reproduction in condition VEST+NECK (head only rotation). However, once  $\dot{ts}$  is large enough to carry the bias across the threshold, Eq. B2 will read:

$$PS=os(1-b\times t)+(TS-ts) \quad (B3)$$

where  $b$  is the coupling coefficient and  $t$  represents the integration time (essentially equal to the duration of the movement). According to Eq. B3, whichever stimulus condition other than VEST+NECK is used, the slope will decrease by a factor of  $b\times t$ , thus explaining the more pronounced effect with 0.1-Hz rotations as compared to 0.8 Hz. Conceivable mechanisms that could justify this rather formalistic explanation have been presented in the Discussion.

### Vestibular noise

If our model of vestibular-neck interaction is to be a realistic representation of biological information processing, it also must be a source of noise, and this noise certainly contributes to the across-trials SD ( $s_{xt}$ ). As explained above (Model), the  $1.2^\circ/s$  threshold effectively blocks the noise as long as there is no supra-threshold  $\dot{ts}$  signal (e.g. during VEST+NECK), whereas with  $TS>1.2^\circ/s$  the noise becomes relevant, riding on top of  $\dot{ts}$  across the threshold.

To confirm these predictions, Monte Carlo simulations of the model were run, in which the variability of the internal estimate of trunk position in space (ts) was analysed as a function of the stimulus frequency for the various stimulus combinations used. For the simulation we assumed independent sources of white noise in the vestibular and dynamic neck proprioceptive channels ( $n_V$  and  $n_N$ , respectively; noise power levels, 0.1). Simulations indicated that the variability of ts rises by a factor of about 6 when stimulation frequency is lowered from 0.8 to 0.1 Hz, with variability for VEST+NECK being always smaller (less than two-thirds) than for all other conditions. The simulations correctly predicted most of the experimentally observed rankings of the four stimulus conditions with regard to  $s_{xt}$  (compare Fig. 4): VEST-NECK>VEST or NECK>VEST+NECK at 0.1 Hz and VEST $\approx$ NECK $\approx$  VEST+NECK at 0.8 Hz; the only non-explained observation being VEST-NECK>All-other-combinations at 0.8 Hz. Finally, when the noise power was increased (more than 0.33), all differences between stimulus conditions disappeared and only the clear dependence on stimulus frequency was retained (note that large noise crosses the threshold even when there is no  $\dot{ts}$  signal).

Originally, our vestibular-neck model was developed to describe various perceptions of self-rotation, but not their variability (Mergner et al. 1991). Its structure was preferred for its parsimony and interpretative power to an alternative one, in which the order of first establishing

a notion ts and subsequently hs (ts + ht) would be reversed (first hs and then ts). Other researchers, who considered somatosensory control of body movements, have focused on “proprioceptive acuity” and inferred from a presumed negative gradient from neck (high acuity) to leg (low) that this control should start with the head and end with the foot (Loeb and Richmond 1999). It was rewarding, therefore, to see that the structure in Fig. 6a correctly predicted the observed variability, unlike the mentioned alternative (ascertained by corresponding simulations).

## References

- Andersen RA, Essick GK, Siegel RM (1985) Encoding of spatial location by posterior parietal neurons. *Science* 230:456–458
- Andersen RA, Bracewell RM, Barash S, Gnadt JW, Fogassi L (1990) Eye position effects on visual, memory, and saccade-related activity in areas LIP and 7a of macaque. *J Neurosci* 10:1176–1196
- Andersen RA, Snyder LH, Li CS, Stricanne B (1993) Coordinate transformations in the representation of spatial information. *Curr Opin Neurobiol* 3:171–176
- Bloomberg J, Melvill Jones G, Segal B, McFarlane S, Soul J (1988) Vestibular-contingent voluntary saccades based on cognitive estimates of remembered vestibular information. *Adv Otorhinolaryngol* 41:71–75
- Blouin J, Gauthier GM, Vercher JL (1997) Visual object localization through vestibular and neck inputs. 2. Updating off-mid-sagittal-plane target positions. *J Vestib Res* 7:137–43
- Blouin J, Labrousse L, Simoneau M, Vercher JL, Gauthier GM (1998a) Updating visual space during passive and voluntary head-in-space movements. *Exp Brain Res* 122:93–100
- Blouin J, Okada T, Wolsley C, Bronstein A (1998b) Encoding target-trunk relative position: cervical versus vestibular contribution. *Exp Brain Res* 122:101–107
- Bock O (1986) Contribution of retinal versus extraretinal signals towards visual localization in goal-directed movements. *Exp Brain Res* 64:467–481
- Bremmer F (2000) Eye position effects in macaque area V4. *Neuroreport* 11:1277–1283
- Enright JP (1995) The non-visual impact of eye orientation on eye-hand coordination. *Vision Res* 35:1611–1618
- Fernandez C, Goldberg JM (1971) Physiology of peripheral neurons innervating semicircular canals of the squirrel monkey. II. Response to sinusoidal stimulation and dynamics of peripheral vestibular system. *J Neurophysiol* 34:661–675
- Henriques DY, Klier EM, Smith MA, Lowy D, Crawford JD (1998) Gaze-centered remapping of remembered visual space in an open-loop pointing task. *J Neurosci* 18:1583–1594
- Howard IP (1982) *Human visual orientation*. Wiley, New York
- Israel I, Berthoz A (1989) Contribution of the otoliths to the calculation of linear displacement. *J Neurophysiol* 62:247–263
- Karn KS, Moller P, Hayhoe M (1997) Reference frames in saccadic targeting. *Exp Brain Res* 115:267–282
- Lewald J, Ehrenstein WH (2000) Visual and proprioceptive shifts in perceived egocentric direction induced by eye-position. *Vision Res* 40:539–547
- Loeb GE, Richmond FJR (1999) Is the neck a leg? *Abstr IVth Int Symp Head/Neck System*, Tokyo, August 22–25. Tokyo Medical University, Tokyo, p 16
- Mapp AP, Barbeito R, Bedell HE, Ono H (1989) Visual localization of briefly presented peripheral targets. *Biol Cybern* 60:261–265
- Maurer C, Kimmig H, Trefzer A, Mergner T (1997) Visual object localization through vestibular and neck inputs. I. Localization with respect to space and relative to the head and trunk mid-sagittal planes. *J Vestib Res* 7:113–135
- Mergner T, Rosemeier T (1998) Interaction of vestibular, somatosensory and visual signals for posture control and motion perception under terrestrial and microgravity conditions. *Brain Res Rev* 28:118–135
- Mergner T, Siebold C, Schweigart G, Becker W (1991) Human perception of horizontal trunk and head rotation in space during vestibular and neck stimulation. *Exp Brain Res* 85:389–404
- Mergner T, Rottler G, Kimmig H, Becker W (1992) Role of vestibular and neck inputs for the perception of object motion in space. *Exp Brain Res* 89:655–668
- Mergner T, Huber W, Becker W (1997) Vestibular-neck interaction and transformation of sensory coordinates. *J Vestib Res* 7:347–367
- Mergner T, Nasios G, Anastasopoulos D (1998) Vestibular memory-contingent saccades involve somatosensory input from the body support. *Neuroreport* 9:1469–1473
- Mergner T, Schweigart G, Müller M, Hlavacka F, and Becker W (2000) Visual contributions to human self-motion perception during horizontal body rotation. *Arch Ital Biol* 138:139–166
- Moshovakis AK, Highstein SM (1994) The anatomy and physiology of primate neurons that control rapid eye movements. *Annu Rev Neurosci* 17:465–488
- Müller GE (1916) Über das Aubertsche Phänomen. *Z Sinnesphysiol* 49:109–246
- Nasios G, Rumberger A, Maurer C, Mergner T (1999) Updating the location of visual objects in space following vestibular stimulation. In: Becker W, Deubel H, Mergner T (eds) *Current oculomotor research – physiological and psychological aspects*. Plenum, New York, pp 203–212
- Pouget A, Snyder LH (2000) Computational approaches to sensorimotor transformations. *Nat Neurosci [Suppl]* 3:1192–1198
- Prablanc C, Echallier JF, Komilis E, Jeannerod M (1979) Optimal response of eye and hand motor systems in pointing at a visual target. *Biol Cybern* 35:113–124
- Schall JD (1995) Neural basis of saccade target selection. *Rev Neurosci* 6:63–85
- Skavenski AA, Steinman RM (1970) Control of eye position in the dark. *Vision Res* 10:193–203
- White JM, Levi DM, Aitseaomo AP (1992) Spatial localization without visual references. *Vision Res* 32:513–526
- White JM, Sparks DL, Stanford TR (1994) Saccades to remembered target locations: an analysis of systematic and variable errors. *Vision Res* 34:79–93